# Obesity and brain topological organization differences throughout the lifespan.

**Ottino-González, J.[1,2,3,*], Baggio, H.C.[2,4,*], Jurado, M.A.[1,2,3,✉], Segura, B.[2,4], Caldú, X.[1,2,3], Prats-Soteras, X.[1,2,3], Tor, C.[7], Sender-Palacios, M.J.[7], Miró, N.[6], Sánchez-Garre, C.[6], Dadar, M.[5], Dagher, A.[5], García-García, I.[5], and Garolera, M.[8,9]**

[1]Departament de Psicologia Clínica i Psicobiologia. Universitat de Barcelona, Spain.
[2]Institut de Neurociències. Universitat de Barcelona, Spain.
[3]Institut de Recerca Sant Joan de Dèu. Hospital Sant Joan de Dèu, Spain.
[4]Departament de Medicina. Universitat de Barcelona, Spain.
[5]Montreal Neurological Institute. McGill University, Canada.
[6]Unitat de Endocrinologia, Hospital de Terrassa. Consorci Sanitari de Terrassa, Spain.
[7]CAP Terrassa Nord. Consorci Sanitari de Terrassa, Spain.
[8]Unitat de Neuropsicologia, Hospital de Terrassa. Consorci Sanitari de Terrassa, Spain.
[9]Brain, Cognition and Behaviour Research Group. Consorci Sanitari de Terrassa, Spain.
[*]These authors contributed equally to this work.

**Life expectancy and obesity rates have drastically increased in recent years. An unhealthy weight is related to long-lasting biological deregulations that might compromise the normal course of development and the so-called "successful aging". The aim of the current study was to test whether an obesity status could mimic the functional organization of an otherwise healthy aged brain. To this end, we included adults with (N = 32, mean age 34.5 ± 6.49) and without obesity (N = 34, mean age 32.7 ± 6.79) as well as adolescents with obesity (N = 30, mean age 15.3 ± 2.64) and normal-weight (N = 31, mean age 15.6 ± 2.60). A sample of stroke-free non-obese and non-demented seniors was also entered (N = 32, mean age 66.1 ± 7.43). Participants underwent a resting-state MRI acquisition and graph-based measurements of segregation, integration and robustness (i.e., mean degree and strength) were calculated. Obesity in adults was accompanied by a broad pattern of losses in network robustness when compared to healthy-weight adults and seniors, as well as increases in network segregation relative to elders. Differences in adolescents followed the same direction yet did not survive multiple comparison adjustment. No interaction emerged when exploring the transition from childhood to adulthood accounting for body-weight status. While more research is needed, we offer preliminary evidence of an obesity status negatively rendering network resilience, which could compromise the normal course of aging.**

**Obesity | Aging | Maturation | Resting-state | Graph-theory**
**Correspondence:** ***majurado@ub.edu***

## Introduction

Our life expectancy is longer than it has ever been before. Above 30% of the population from Western developed countries will be older than 60 years by 2050 (World Health Organization, 2015). For this reason, research on the psychobiological factors that have an impact on the so-called "successful aging" is rapidly gaining popularity. One of such factors is obesity. The World Health Organization (WHO) estimates that the prevalence of obesity has tripled in the last decades (WHO, 2017). Particularly, children and teenagers with obesity represent a serious matter of concern as they are most likely to stay overweight throughout life and develop long-lasting medical comorbidities earlier than adults (WHO, 2018). The far-reaching consequences of obesity involve several chronic conditions, such as type II diabetes, cardiovascular diseases and cancer (Wade, Carslake, Sattar, Davey Smith, & Timpson, 2018). On a similar note, obesity could accelerate brain aging (Ronan et al., 2016; Tzanetakou, Katsilambros, Benetos, Mikhailidis, & Perrea, 2012), increasing the odds of suffering late-onset dementia (Bischof & Park, 2015). Neuroanatomical studies suggest that obesity is associated with alterations in gray matter (GM) and white matter (WM) composition in both adults (García-García et al., 2018; Repple et al., 2018; Zhang et al., 2018) and adolescents (Kennedy, Collins, & Luciana, 2016; Ou, Andres, Pivik, Cleves, & Badger, 2015). Thus, morphologically at least, this condition could induce changes in the brain that resemble those prompted by aging.

The functional organization of the brain is intricate. Distinct and anatomically distant regions interact with each other contributing to cognitive function. Graph-based indexes could serve as proxies of the complex rendering of large-scale networks. Measures of segregation, such as modularity, represent how neighboring nodes tend to aggregate as independent clusters (Rubinov & Sporns, 2010). This community-based organization underpins the principle of brain economics with highly specialized modules dedicated to the processing of certain sources of information, mostly of sensory nature (Wig, 2017). Integration indexes reflect instead to which extent a priori unrelated modules interchange information. A typical surrogate of integration is the characteristic path length (path length, from now on). This parameter echoes the shortest path between modules (Rubinov & Sporns, 2010). Hence, the fewer the jumps, the greater the integration between communities. Well-balanced short and long-range connections allow the rapid combination of resources necessary for higher cognitive activity. Finally, degree and strength mirror the network integrity and efficiency by averaging the amount and the weight of connections a given node has with the rest of the brain (Rubinov & Sporns, 2010). Densely interconnected nodes are metabolically costly and commonly referred to as "hubs" as they exert as bridges coupling remote clusters (van den Heuvel & Sporns, 2013).

DRAFT

Aging is associated with losses in the differentiation between well-defined circuits. Independent clusters tend to enhance their between-cluster communications at the expense of their within-cluster interactions. In other words, aging is associated with decreases in modularity (Geerligs, Renken, Saliasi, Maurits, & Lorist, 2015) and increases in path length (Sun, Tong, & Yang, 2012). These losses in network discreteness could reflect nodal strength reductions as well as trimming or weakening of short-range connections (i.e., drops in degree and strength) (Sala-Llonch et al., 2014). Similarly, during childhood and adolescence, the brain progressively steps from highly clustered and randomly wired communities towards less modular and better connected ones (Boersma et al., 2013). These are thought to reveal age-related changes within GM/WM tissues (e.g., axonal pruning, cell-shrinkage) (Cao et al., 2014).

To date, and to the best of our knowledge, only four studies have explored the brain functional organization in obese individuals with graph-theoretical parameters, with three of them conducted in adults. The first two reported lower modularity in individuals with obesity when compared to healthy-weight subjects (Baek, Morris, Kundu, & Voon, 2017; Chao et al., 2018). The third and fourth study described global brain connectivity decreases mainly among prefrontal circuits in both adults and adolescents (Geha, Cecchi, Todd Constable, Abdallah, & Small, 2017; Moreno-Lopez, Contreras-Rodriguez, Soriano-Mas, Stamatakis, & Verdejo-Garcia, 2016). As mentioned above, decreases in modularity and network robustness might in turn be symptomatic of premature aging as these features are typical of the elderly. Because of these observations and their potential long-term consequences over health, the current study had two aims. The first and main objective was to compare the brain connectivity organization of adults with and without obesity to otherwise healthy elders. We further expect analogous connectivity profiles between adults with obesity and seniors. The second aim was to test whether the differences in adults relative to their bodyweight status would be noticeable earlier in life. To this end, we compared adolescents with and without obesity presuming similar results as in the adults' contrast. A supplemental objective of this study was to explore whether an obesity status could differently shape the brain topological organization during maturation, or the transition from childhood to adulthood.

## Methods

**Participants.** Two independently collected samples were included in this work. One sample comprised 32 non-obese healthy seniors (51-85 years old). The recruitment procedure of this group is fully described in Abós et al. (2017). Briefly, exclusion criteria consisted on presence of psychiatric or neurological comorbidity, low global intelligence quotient estimated by the WAIS-III Vocabulary subtest score (> 7 scalar score) (Wechsler, 1999), and a Mini-Mental state examination score below 25 (Folstein, Folstein, & McHugh, 1975). For the current work, senior participants with obesity (body mass index [BMI] equal to or higher than 30 kg/m$^2$) were excluded (N = 4) as well as those presenting MRI pathological findings such as white matter hyperintensities unrelated to the course of normal aging (N = 2).

The other sample included 61 adolescents (12-21 years old) and 66 adults (22-48 years old) from public health care centers belonging to the *Consorci Sanitari de Terrassa*. This sample was recruited in the context of a broader line of research revolving around obesity and brain function. Part of this sample was used in previous works (Ariza et al., 2012; Caldú et al., 2019; García-García et al., 2013a, 2013b, 2013c, 2015; Marqués-Iturria et al., 2013, 2014, 2015; Ottino-González et al., 2017, 2018, 2019). Thirty-two adults were considered as obese and 34 as normal weight (BMI < 24.9 kg/m$^2$). Following the cut-offs established by the WHO (2012), 30 adolescents above the gender-based 95$^{th}$ BMI percentile were categorized as obese, and 31 teens oscillating between the 5$^{th}$ and the 84$^{th}$ percentile were categorized as healthy-weight (Cole, Flegal, Nicholls, & Jackson, 2007).

Thirty-four individuals with overweight (i.e., BMI 25 kg/m$^2$ to 29.9 kg/m$^2$, or between the 85$^{th}$ and 94$^{th}$ percentiles for adolescents) were not included in this study. Here, we were interested in addressing the two extremes of the BMI continuum, since including overweight subjects could introduce unwanted artefacts. For instance, the presence of normal-weight obese individuals (i.e., healthy-weight participants exhibiting excessive abdominal adiposity) or athletic-like persons misclassified as overweight according to their BMI.

As in previous work, we excluded participants with cardiometabolic comorbidities (i.e., type II diabetes, hypercholesterolemia, hypertension), as well as those with past or present neurological or psychiatric disorders. Individuals underwent three visits. The first consisted of a fasting blood sample extraction and a medical exploration. The second visit included an extensive neuropsychological evaluation in which subjects with a Vocabulary subtest scalar score below 7 were discarded (WAIS-III or WISC-IV) (Wechsler, 1999, 2007). The third and last visit comprised a magnetic resonance imaging (MRI) acquisition at the *Hospital Clínic de Barcelona*.

Additionally, participants from all five groups exhibiting excessive head motion were discarded (N = 16). Excessive movement was defined as (1) mean interframe head motion greater than 0.3 mm translation or 0.3° rotation, and (2) maximum interframe head motion greater than 1 mm translation or 1° rotation.

**MRI acquisition.** Images were acquired with a 3T Siemens scanner (MAGNETOM Trio, Siemens, Germany). Each participant underwent a T1-weighted structural image for co-registration and parcellation purposes with the MPRAGE-3D protocol [echo time (TE) = 2.98 ms; repetition time (TR) = 2300 ms; inversion time = 900 ms; 256 mm field of view [FOV]; matrix size = 256 x 256; voxel size = 1.0 x 1.0 x 1.0 mm$^3$). Resting-state volumes were collected using a multi-slice gradient-echo EPI sequence covering the whole brain (TE = 19 ms; TR = 2000 ms; 3 mm slice thickness; 90° flip angle; 220 mm FOV; voxel size = 1.7 x 1.7 x 3.0 mm$^3$).

DRAFT

**Image pre-processing.** Basic functional image preprocessing, using AFNI (http://afni.nimh.nih.gov/afni) and FSL (https://www.fmrib.ox.ac.uk/fsl) tools, included: discarding the first five volumes to allow magnetization stabilization, despiking, motion correction, brain extraction, grand-mean scaling (to keep signal variation homogeneous across subjects), linear detrending, and high-pass filtering (maintaining frequencies above 0.01 Hz). Functional images and T1-weighted volumes were co-registered and then non-linearly normalized to the MNI ICBM152 template. Then, images were non-linearly transformed to MNI space at 3 x 3 x 3 $mm^3$ voxel size using SPM (http://www.fil.ion.ucl.ac.uk/spm/).

To remove the effects of head motion and other non-neural sources of signal variation from the functional data sets, we used an independent component analysis (ICA)-based strategy for Automatic Removal of Motion Artifacts (ICA-AROMA) (Pruim et al., 2015). This method uses individual resting-state data to perform ICAs and automatically identify artifact-related independent components. The time courses of components considered as artifactual were stored to be used as regressors during network computation.

The six motion parameters obtained from the realignment procedure, as well as the average white matter and cerebrospinal fluid signals were kept as regressors in network reconstruction. To generate the corresponding white matter and cerebrospinal fluid (lateral ventricle) masks, T1-weighted structural images were segmented using FreeSurfer (https://surfer.nmr.mgh.harvard.edu/). The resulting binary masks were linearly transformed from structural to native functional space using FSL-FLIRT (https://fsl.fmrib.ox.ac.uk/fsl/fslwiki/FLIRT). To prevent these masks from extending to the adjacent gray matter due to resampling blur in linear transformation, white matter masks were then "eroded" by applying a threshold of 0.9, while ventricular masks were thresholded at 0.3.

**Connectivity matrix computation.** To reconstruct the functional connectome, the brain needs to be divided into a set of nodes; network edges connecting pairs of nodes are then defined as a measure of relationship between their respective time courses. In this work, we used the Brainnetome atlas (Fan et al., 2016), a cross-validated connectivity-based parcellation scheme that divides the cerebrum into 210 cortical and 36 subcortical gray matter regions, taken as network nodes. To reflect the main dimension of signal variation across each region (Friston et al., 2006), the first eigenvariates of the time series of all voxels included in each region mask were extracted using *fslmeants* and taken as the time course of the corresponding nodes.

Individual 246 x 246 connectivity matrices were then reconstructed by calculating the standardized regression coefficient between the time courses of nodes *i* and *j*, while also entering the ICA-AROMA artifact time courses, six motion parameters, and white matter and cerebrospinal fluid mean time courses as regressors. This produces fully connected and undirected brain networks with 30,135 unique edges with values ranging between -1 and 1.

Moreover, a group temporal-concatenation spatial ICA was performed using FSL's MELODIC (https://fsl.fmrib.ox.ac.uk/fsl/fslwiki/MELODIC) with a pre-determined dimensionality of 15 independent components. The spatial and power spectral characteristics of the resulting components were inspected to identify 10 well-established networks (Griffanti et al., 2017): two primary visual networks (PVN and PVN2), secondary visual network (SVN), default mode network (DMN), dorsal attentional network (DAN), anterior default mode network (aDMN), right and left frontoparietal networks (FPN), sensory-motor network (SM) and the salience network (SN) (see Supplementary Figure 1). Two additional networks were identified as the medial temporal network (MTN) (including the hippocampus and the amygdala) and the striatal-thalamic network (STN).

These data-driven spatial maps were used to assign the Brainnetome's nodes to specific brain networks for further regional graph-based measurements calculation, using in-house MATLAB scripts. Specifically, the Z-maps generated by MELODIC corresponding to the 12 networks of interest were thresholded at $Z \geq 2$. Subsequently, each Brainnetome node was considered to belong to a network if over 60% of its voxels overlapped with this network's thresholded map. When this overlap occurred for more than one network, the sum of the Z-values across all overlapping voxels was considered, and the node was assigned to the network with the highest Z-value sum. In total, 153 of the 246 Brainnetome nodes were ascribed to one of the 12 networks of interest, as shown in Supplementary Table 1.

**Global and regional measurements estimation.** Global network parameters were computed using the Brain Connectivity Toolbox (Rubinov & Sporns, 2010) and in-house MATLAB scripts.

Normalized weighted global measures were computed by averaging the ratio between the actual measure and those obtained through randomly rewiring the connectivity matrix 500 times using Maslov-Sneppen's degree-preserving algorithm. After setting negative edge weights to zero, we computed the characteristic path length, defined as the average minimum number of edges that need to be traversed between each pair of network nodes (Rubinov & Sporns, 2010).

As non-normalized global parameters, the modularity coefficient was estimated using the Louvain algorithm and indicating the degree to which a network can be subdivided into well-defined modules with few intermodular connections. This was also calculated after setting negative edges to zero, but maintaining positive edge weights.

We also assessed two other complementary non-normalized metrics: the mean network degree (i.e., average number of positive connections linked to a node, across all brain nodes) and the mean network strength (i.e., average of unthresholded connection strength across all edges, positive and negative), both of which can be understood as measures of network efficiency and integrity, or robustness. Regional parameters such as nodal degree and strength were calculated by averaging the

DRAFT

total number of connections and weights between nodes ascribed to each ICA-based network and the rest of the brain.

## Statistical analysis

Sociodemographic variables as well as the mean interframe translational and rotational movements of the head were examined across groups. Non-parametrical tests were applied when data assumptions were violated. All comparisons, including post-hoc pairwise contrasts, of both global and regional graph-based measures were conducted with permutation-based tests (10,000 permutations).

One-factor univariate general linear models (GLMs) were conducted in adults and seniors. To avoid comparisons of non-interest, differences in adolescents were tested in independent models. Post-hoc pairwise t-tests were performed for contrasts that emerged as statistically significant. Cumulative odds for false-positive results were prevented with Bonferroni-adjustments. Here, the raw p-values were multiplied by *k* variables for omnibus tests (i.e., by 4 for global graph-based measures, and by 12 for regional degree and strength parameters), and by *n* contrast of interest (e.g., adults with obesity vs. healthy-weight adults, adults with obesity vs. seniors and healthy-weight adults vs. seniors) in post-hoc comparisons. Statistical significance was set at Bonferroni-adjusted p-value < 0.05. Likewise, effect sizes (i.e., Cohen's d [d] or eta-partial squared [$\eta p^2$]) and bias-corrected and accelerated bootstrap (10,000 simulations) confidence intervals (CI) at 95% (90% for two-factor ANCOVAs) were calculated for each significant pairwise contrast.

Moreover, and apart from body-weight status (i.e., healthy-weight vs obesity) main effects, we explore interactions between the former and developmental stage (i.e., adult vs adolescent) with two-factor univariate GLMs. All statistical analyses were performed with *R* version 3.5.0 (R Core Team, 2018).

## Results

**Sociodemographics.** As expected, groups differed in age ($F_{(4,153)}$ = 420, p < 0.001) and years of education ($F_{(4,153)}$ = 24.62 p < 0.001). Post-hoc tests revealed no significant differences between adults with and without obesity in age (p-adjusted = 0.674) or education (p-adjusted = 0.854). Similarly, healthy-weight and obese adolescents were comparable in terms of age (p-adjusted = 0.999) and years of education (p-adjusted = 0.732). All five groups were equally distributed for sex ($x^2$ = 1.22, p = 0.875) (see summary in Table 1).

**Table 1.** Sociodemographics across groups (mean and standard deviation)

| Groups | Age | Education | N/Females |
|---|---|---|---|
| OB adult | 34.53 (6.49) | 13.88 (2.92) | 32/20 |
| HW adult | 32.68 (6.79) | 14.62 (2.75) | 34/18 |
| Senior | 66.13 (7.43) | 11.22 (4.26) | 32/17 |
| OB young | 15.27 (2.64) | 8.57 (2.45) | 30/15 |
| HW young | 15.64 (2.60) | 9.52 (2.19) | 31/16 |

OB = participant with obesity, HW = healthy-weight individual.

**MRI quality check.** Rotational movements of the head did not diverge between groups ($H_{(4)}$ = 4.32, p = 0.364). By contrast, head translational movements did prove different ($H_{(4)}$ = 38.90, p < 0.001). Post-hoc contrasts revealed that such displacements were more marked for elders and adults with obesity, as both of them differed from the other groups yet not from each other. Consequently, head translational movements were controlled for all further graph-theoretical analyses including these groups, either by introducing it as a covariate or by regressing out its effects from the variable of interest.

**Global graph-based results.** Adults and seniors exhibited differences in modularity ($F_{(3,94)}$ = 5.71, p-adjusted = 0.020), mean degree ($F_{(3,94)}$ = 5.56, p-adjusted = 0.024), and mean strength ($F_{(3,94)}$ = 4.81, p-adjusted = 0.039).

Post-hoc tests exposed that the contrast between adults with obesity and without did not pass the Bonferroni adjustment (raw p-value = 0.024). Still, individuals with obesity showed lower mean degree (t = 2.69, p-adjusted = 0.012, d = -0.66; $CI_{bca}$95% [-1.11, -0.19]) and mean strength (t = 2.74, p-adjusted = 0.015, d = -0.68; $CI_{bca}$95% [-1.10, -0.21]) when compared to their normal-weight counterparts. Relative to seniors, adults with obesity presented greater modularity (t = -3.94, p-adjusted = 0.002, d = 0.99; $CI_{bca}$95% [0.45, 1.55]), as well as lower mean degree (t = 3.38 , p-adjusted = 0.007, d = -0.85; $CI_{bca}$95% [-1.32, -0.37]) and strength (t = 2.81, p-adjusted = 0.025, d = -0.70; $CI_{bca}$95% [-1.16, -0.22]). Normal-weight adults did not differ from non-obese elders for any of the abovementioned. Results are depicted below in Figure 1.

While analogous to adults, differences in adolescents in mean degree and strength did not survive multiple comparison correction (0.034 and 0.033, raw p-values for each contrast) (see Figure 3 and Figure 4). Additionally, mean and standard deviation across groups for graph-based parameters are included in the Supplementary Table 2.

**Regional nodal degree and strength results.** Adults and seniors diverged in the average number of inward and outward connections in the DMN ($F_{(3,94)}$ = 5.97, p-adjusted = 0.048). Here, adults with obesity displayed lesser regional degree than healthy-weight adults in the DMN (t = 3.21, p-adjusted = 0.008, d = -0.79; $CI_{bca}$95% [-1.26 -0.33]) and seniors( t = 3.15, p-adjusted = 0.007, d = -0.79; $CI_{bca}$95% [-1.26 -0.28]).

Groups also diverged in the DMN strength connectivity ($F_{(3,94)}$ = 7.02, p-adjusted = 0.022). Adults with obesity demonstrated lower strength when rivalled against their healthy-weight peers (t = 3.67, p-adjusted = 0.001, d = -0.90; $CI_{bca}$95% [-1.33, -0.44]) and non-obese elders (t = 2.57, p-adjusted = 0.031, d = -0.64; $CI_{bca}$95% [-1.03, -0.17]). Healthy-weight adults did not prove different from seniors neither for degree nor strength in the DMN (see Figure 3).

What is more, differences in the regional degree ($F_{(3,94)}$ = 6.61, p-adjusted = 0.008) emerged in the SMN. In contrast to healthy-weight adults, adults with obesity revealed

DRAFT

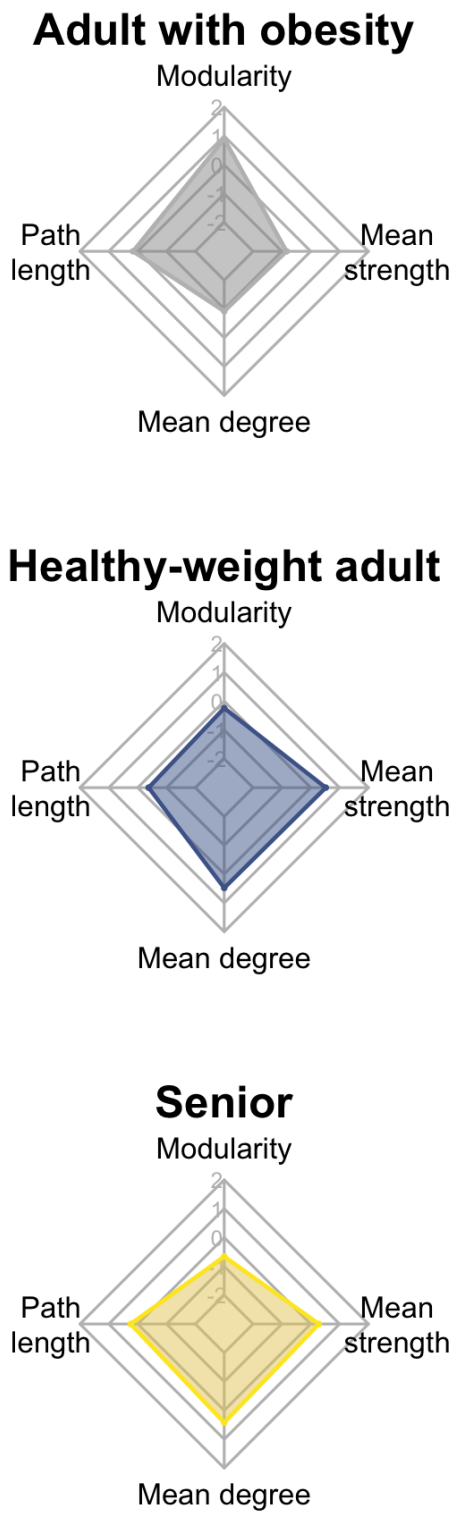


**Figure 1**. Network profiles of adults with obesity, healthy-weight adults and seniors.

lesser nodal degree (t = 3.45, p-adjusted = 0.005, d = -0.85; $CI_{bca}$95% [-1.35, -0.36]). The contrast from adults with obesity and elders did not survive Bonferroni adjustment (raw p-value = 0.041). Groups also differed in the SMN

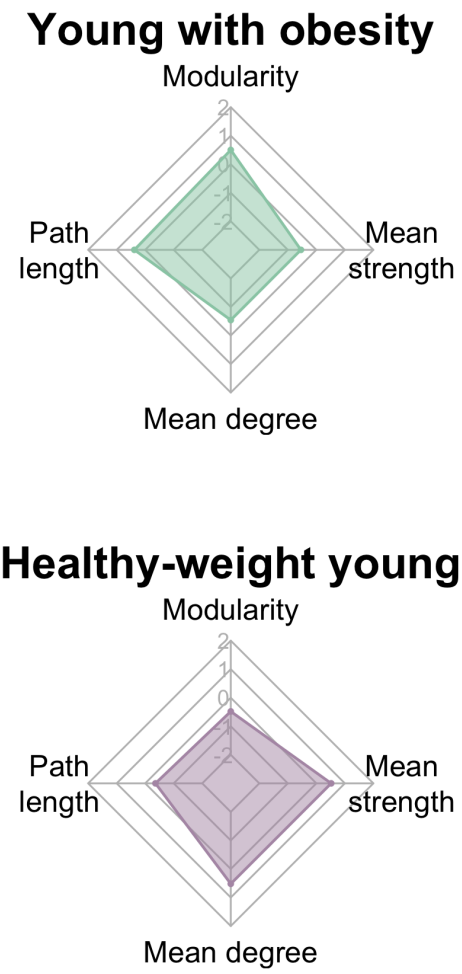


**Figure 2**. Network profiles of adolescents with and without obesity.

strength ($F_{(3,94)}$ = 6.23, p-adjusted = 0.031). Adults with obesity did also show lesser strength than healthy-weight adults within this network (t = 3.54, p-adjusted = 0.002, d = -0.87; $CI_{bca}$95% [-1.37, -0.38]). The contrast between this group and elders did not emerge as statistically significant. Adults without obesity did not differ from seniors for any measure of the SMN. Results are displayed in Figure 4.

Adolescents with and without obesity only proved different in the regional degree (t = 2.98, p-adjusted = 0.043, d = -0.76; $CI_{bca}$95% [-1.27 -0.24]) and strength (t = 3.10, p-adjusted = 0.041, d = -0.79; $CI_{bca}$95% [-1.31 -0.24]) of the PVN (see Figure 5).

**Body-weight status and age interaction.** There were no significant interactions between body-weight status and age for any graph-theoretical measurement as presented in Figure 6. No interaction emerged for regional indexes either. Independent of age, participants with obesity differed from their healthy-weight peers in modularity ($F_{(1,122)}$ = 11.08, p-adjusted = 0.005, $\eta p^2$ = 0.074, $CI_{bca}$90%[0.02 0.16]), mean degree ($F_{(1,122)}$ = 12.95, p-adjusted < 0.001, $\eta p^2$ = 0.080, $CI_{bca}$90% [0.02 0.16]) and mean strength ($F_{(1,122)}$ = 12.25,

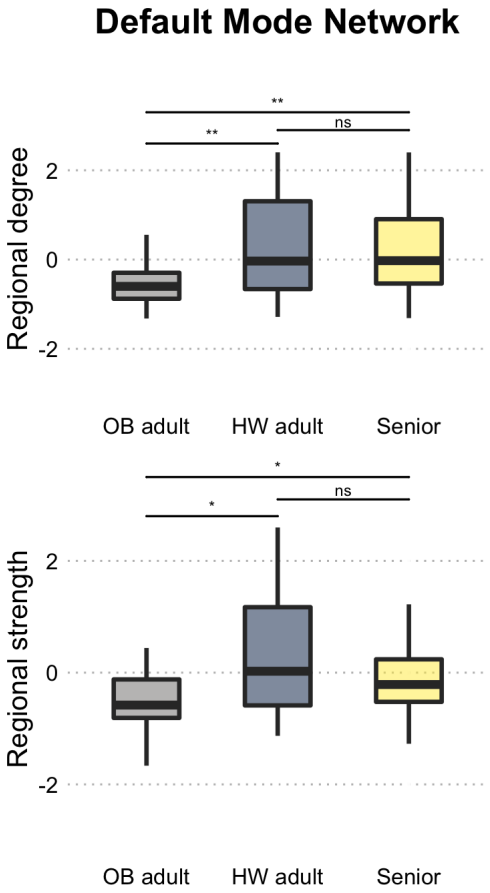


**Figure 3**. Group comparison for DMN regional degree and strength. OB = participants with obesity, HW = healthy-weight individuals, *<0.05, **<0.01, ns = non-significant.

p-adjusted < 0.001, $\eta p^2 = 0.094$, $CI_{bca}90\%[0.03 \quad 0.18]$).

## Discussion

Obesity is a preventable health problem associated with the development of long-lasting cardiometabolic disorders (Wade et al., 2018) and late-onset dementia (Bischof & Park, 2015; Deckers, van Boxtel, Verhey, & Köhler, 2017). The current work aimed to shed a broader light on whether the network profile of adults with obesity could mirror the typical rendering seen in the elderly. Likewise, we intended to extend the findings described in adults with and without obesity to adolescents. Lastly, we explored whether an obesity status could differently shape the rendering of large-scale networks when moving from childhood to adulthood. Regarding the first objective, and contrary to what was initially postulated, adults with obesity differed from the group of elders. Participants with obesity demonstrated greater modularity in comparison to the later. Moreover, individuals with obesity exhibited lower mean degree and strength not only when compared to non-obese seniors but also to healthy-weight adults. Still, some of these findings stood in line with the literature, which might suggest that some aging-related features might be intensified in adults with obesity. Strikingly, normal-weight adults did not diverge from seniors in any graph-theoretical parameter. Speculations on such inconsistency with seminal works are further discussed in this section. In relation to the second aim, differences between youngsters did not pass multiple comparison corrections for global properties but for regional ones. Concretely, adolescents with obesity exhibited differences in visual-related networks. Lack of results in global-based parameters will be disclosed separately for this group. Finally, no interaction emerged as significant between body-weight status and developmental stage for any of the abovementioned.

**Modularity.** This index can be generally regarded as a proxy of network segregation, which stands for how clustered the brain is in terms of sharing and processing information (Sporns, 2013). Adults with obesity showed a pattern of enhanced cliquishness relative to seniors (and healthy-weight adults to some extent) with relatively large effect sizes. The increases in segregation are in contrast to what has been portrayed in previous obesity work (Baek et al., 2017; Chao et al., 2018). Nevertheless, it is also fair to point out that those studies were conducted in individuals diagnosed with eating disorders or in seeking for treatment (i.e., bariatric surgery). None of the subjects included had any psychiatric diagnosis nor were recruited for treatment purposes. In connection to the aim of the current study, the network profile we found is the opposite of what is described in the elderly. As the brain

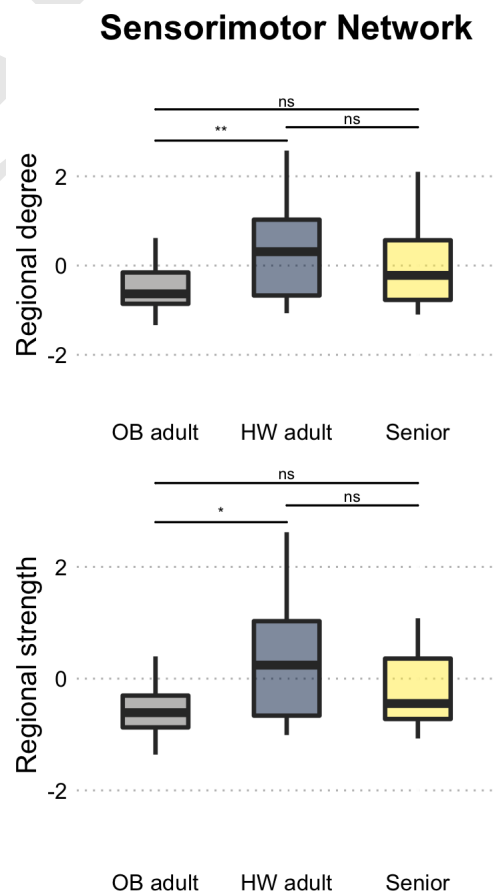


**Figure 4**. Group comparison for SMN regional degree and strength. OB = participants with obesity, HW = healthy-weight individuals, *<0.05, **<0.01, ns = non-significant.

DRAFT

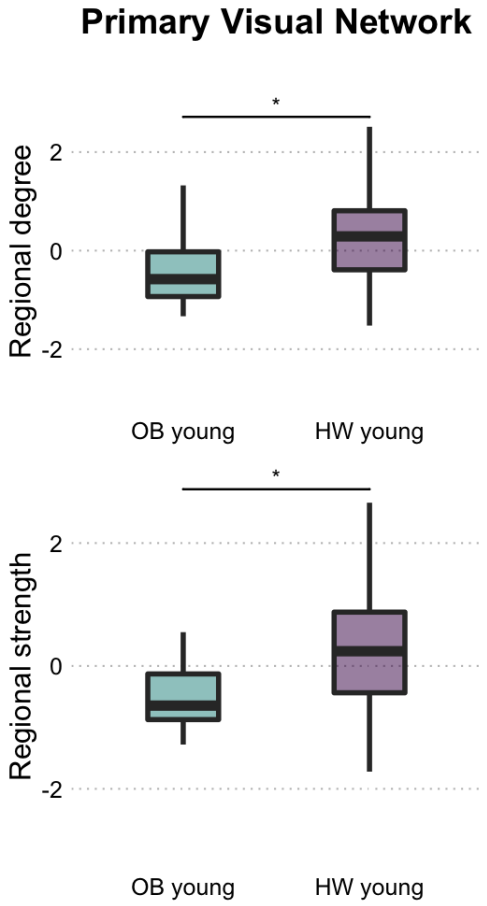


**Figure 5**. Group comparison for PVN regional degree and strength. OB = participants with obesity, HW = healthy-weight individuals, *<0.05.

ages, modularity tends to decrease (Cao et al., 2014), which can be a consequence from the progressive scattering of intra-network connections (Geerligs et al., 2015; Sala-Llonch, Bartrés-Faz, & Junqué, 2015; Sala-Llonch et al., 2014). Although such configuration could benefit the processing of sensory-specific information, higher-level cognitive activity may in turn deteriorate (Sporns, 2013). Excessively isolated clusters would not be able to exchange information efficiently. This finding may relate to the well-known increment in the processing times that elders and subjects with obesity tend to show in their cognitive performance (Deckers et al., 2017; Sala-Llonch et al., 2014). Also, an escalation in modularity could entail a vulnerability to cardiovascular-related disconnection syndromes (e.g., aphasia) (Siegel et al., 2018). It is widely acknowledged that obesity constitutes a risk factor for coronary heart disease, cerebrovascular disease and heart failure, even among those metabolically healthy (Caleyachetty et al., 2017). In fact, it is very likely that obese individuals presenting a relatively favorable health condition will qualify as unhealthy later in life (Mongraw-Chaffin et al., 2016). That said, the large-scale network configuration here described admits a second lecture; being obese may represent a downside in the face of cardiovascular events potentially happening during the course of aging.

**Global and regional mean degree and strength.** These parameters, respectively, mirror the number of edges connected to a given node and the average weight of such links. Therefore, both return a global reading of the network integrity and efficiency, or robustness. Our results showed that adults with obesity revealed a lower mean degree and strength when compared to healthy-weight adults with effect sizes ranging from medium to large. These results are partially in line with the study conducted by Geha et al. (2017). In this work, the authors presented a measure of global brain connectivity, defined as the number of connections each node has with others. As mentioned above, one of the consequences of aging on the brain is the trimming of short-range edges and the scattering of nodes (Sala-Llonch et al., 2014). Individuals with obesity did show losses in overall network robustness. This increase in network frailty could indeed be echoing symptoms of premature aging (Geerligs et al., 2015; Sala-Llonch et al., 2015, 2014).

What is more, when examined regionally, we found group differences in sensory-driven (i.e., SMN) and task-negative networks (i.e., DMN), which support our previous findings suggesting reductions in whole-brain network-resilience. In addition, adolescents with obesity presented lower degree and strength in primary-visual networks (i.e., PVN). The functional properties of sensory-processing circuits (e.g., SMN and PVN) were found to linearly decrease with age (Zonneveld et al., 2019). Other work have also reported that subjects with obesity feature alterations within tactile and visual-processing networks (Doucet et al., 2017; García-García et al., 2013; Geha et al., 2017). Also, the DMN, which is considered as a biomarker for unsuccessful aging

DRAFT

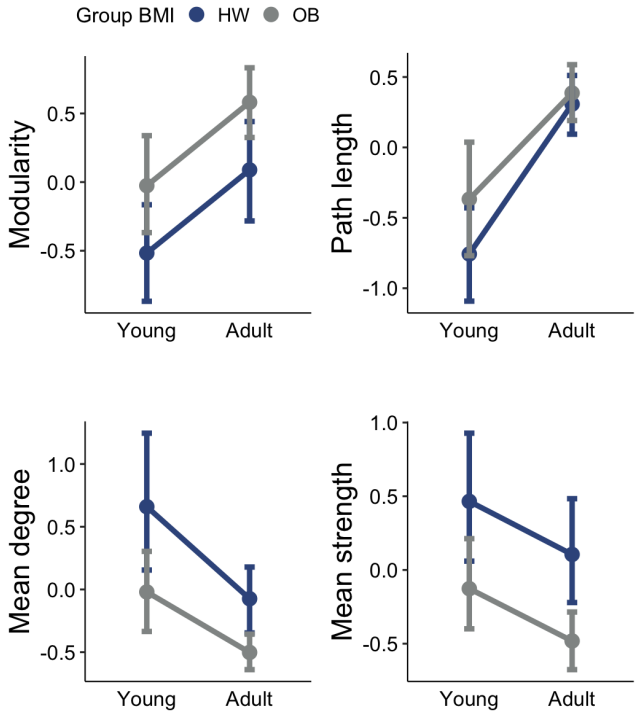


**Figure 6**. Age and body-weight status interactions for global graph-related indexes. OB = participants with obesity, HW = healthy-weight individuals.

(Buckner, Andrews-Hanna, & Schacter, 2008; Palmqvist et al., 2017), is extremely vulnerable to the negative effects of obesity-related comorbidities such as type II diabetes (Wang, Ji, Lu, & Zhang, 2016), hypertension (Haight et al., 2015), and dyslipidemia (Spielberg et al., 2017). To date, few studies have described alterations in the DMN relative to present obesity (Beyer et al., 2017; Doucet et al., 2017; Figley, Asem, Levenbaum, & Courtney, 2016; Tregellas et al., 2011).

Interestingly, no meaningful differences were found between healthy-weight adults and seniors. Literature is consistent in describing modularity reductions in elders (Geerligs et al., 2015; Song et al., 2014), a finding we failed to replicate. Likewise, no differences in network robustness emerged as significant for this contrast. It is important to remark, however, that none of the participants in the senior group was obese, a condition that alone (Beyer et al., 2017; Doucet et al., 2017), or in conjunction with its medical complications (Haight et al., 2015; Spielberg et al., 2017; Wang et al., 2016), proved enough to yield differences in network connectivity. This criterion is often overlooked in healthy-aging literature. Following this line, the seniors' group was also composed by literate individuals, free from stroke and cognitively intact. Although more research is needed, we cannot rule out the possibility that such sample might not have been representative of the elder population. Therefore, some of the results hereby presented should be taken with caution.

Yet analogous to the results in adults, differences in adolescents did not survive multiple comparison correction. Nevertheless, evidence of loses in network robustness in adolescents with obesity are documented in a recent work (Moreno-Lopez et al., 2016). As some of the functional alterations might already be noticeable earlier in life, this contrast should be further tested with enough-powered samples. Here, and regardless of age, individuals with obesity differed from their healthy-weight peers in measures of modularity and network robustness. Put differently, we did not witness an interaction between body-weight status and developmental stage. This supports the idea of obesity impacting brain circuits at very early stages of life. This inference, preliminary as it is, should be properly confirmed with longitudinal studies.

In line with the observations exposed earlier, the current work has limitations that need to be addressed in the future. First, the study's cross-sectional nature precludes concluding upon causality. Longitudinal approaches would help disentangle whether the transition from childhood to adulthood and to elderhood is different in the presence of an unhealthy weight. Second, our modest sample size (N = 159) might have limited our statistical power to catch any subtle disparity between groups (i.e., adolescents with and without obesity contrasts). Third, to have had a group of elders with obesity would have allowed exploring the impact of such condition across all possible age ranges. In the spirit of this, the elders included in this study exhibited some traits (i.e., stroke-free, non-demented and non-obese) that may not fit the natural characteristics of this population. Consequently, we advise reservation upon some of the conclusions here thrown. By contrast, two strong points of this work were the efforts in controlling type I errors and the no inclusion of participants with neurological or psychiatric comorbidities likely prompting differences in network properties (Baek et al., 2017; Chao et al., 2018).

In sum, compared to non-obese seniors, volunteers with obesity exhibited increases in network segregation. Relative to healthy-weight adults and elders, this group also revealed global and regional reductions in network robustness. Overall, an obesity status represents a potentially avoidable hindrance that could negatively affect network resilience. Although more research is needed, this scenario might compromise the normal course of aging in individuals with obesity.

## Bibliography


1. A. Abós, H Baggio, B. Segura, A.I. García-Díaz, Y. Compta, M.J. Martí, F. Valldeoriola, and C. Junqué. Discriminating cognitive status in Parkinson's disease through functional connectomics and machine learning. *Scientific Reports*, 7(1):45347, 12 2017. ISSN 2045-2322. doi: 10.1038/srep45347.
2. M. Ariza, M. Garolera, M.A. Jurado, I. Garcia-Garcia, I. Hernan, C. Sánchez-Garre, M. Vernet-Vernet, M.J. Sender-Palacios, I. Marques-Iturria, R. Pueyo, B. Segura, and A. Narberhaus. Dopamine Genes (DRD2/ANKK1-TaqA1 and DRD4-7R) and Executive Function: Their Interaction with Obesity. *PLoS ONE*, 7(7):e41482, 1 2012. ISSN 1932-6203; 1932-6203. doi: 10.1371/journal.pone.0041482.
3. K. Baek, L. S. Morris, P. Kundu, and V. Voon. Disrupted resting-state brain network properties in obesity: Decreased global and putaminal cortico-striatal network efficiency. *Psychological Medicine*, 47(4):585–596, 2017. ISSN 14698978. doi: 10.1017/S0033291716002646.
4. F. Beyer, S. Kharabian Masouleh, J.M. Huntenburg, L. Lampe, T. Luck, S.G. Riedel-Heller, M. Loeffler, M.L. Schroeter, M. Stumvoll, A. Villringer, and A.V. Witte. Higher body mass index is associated with reduced posterior default mode connectivity in older adults. *Human Brain Mapping*, 3515(April):3502–3515, 2017. ISSN 10970193. doi: 10.1002/hbm.23605.
5. G.N. Bischof and D.C. Park. Obesity and Aging. *Psychosomatic Medicine*, 77(6):697–709, 1 2015. ISSN 0033-3174. doi: 10.1097/PSY.0000000000000212.
6. M. Boersma, D.J.A. Smit, D.I. Boomsma, E.J.C. De Geus, H.A. Delemarre-van de Waal, and C.J. Stam. Growing Trees in Child Brains: Graph Theoretical Analysis of Electroencephalography-Derived Minimum Spanning Tree in 5- and 7-Year-Old Children Reflects Brain Maturation. *Brain Connectivity*, 3(1):50–60, feb 2013. ISSN 2158-0014. doi: 10.1089/brain.2012.0106.
7. R.L. Buckner, J.R. Andrews-Hanna, and D.L. Schacter. The brain's default network: Anatomy, function, and relevance to disease. *Annals of the New York Academy of Sciences*, 1124:1–38, 2008. ISSN 00778923. doi: 10.1196/annals.1440.011.
8. X. Caldú, J. Ottino-González, C. Sánchez-Garre, I. Hernan, E. Tor, M.J. Sender-Palacios, J.C. Dreher, M. Garolera, and M.A. Jurado. Effect of the catechol- O -methyltransferase Val 158 Met polymorphism on theory of mind in obesity. *European Eating Disorders Review*, (August 2018):1–9, 2 2019. ISSN 10724133. doi: 10.1002/erv.2665.
9. S.H. Chao, Y.T. Liao, V.C.H. Chen, C.J. Li, R.S. McIntyre, Y. Lee, and J.C. Weng. Correlation between brain circuit segregation and obesity. *Behavioural Brain Research*, 337(259):218–227, 2018. ISSN 18727549. doi: 10.1016/j.bbr.2017.09.017.
10. T.J Cole, K.M Flegal, S. Nicholls, and A.A Jackson. Body mass index cut offs to define thinness in children and adolescents: international survey. *BMJ (Clinical research ed.)*, 335 (7612):194, 7 2007. ISSN 1468-5833. doi: 10.1136/bmj.39238.399444.55.
11. G.E. Doucet, N. Rasgon, B.S. McEwen, N. Micali, and S. Frangou. Elevated Body Mass Index is Associated with Increased Integration and Reduced Cohesion of Sensory-Driven and Internally Guided Resting-State Functional Brain Networks. *Cerebral Cortex*, (April): 988–997, 2017. ISSN 1047-3211. doi: 10.1093/cercor/bhx008.
12. M.S. Ellulu, I. Patimah, H. Khaza'ai, A. Rahmat, and Y. Abed. Obesity and inflammation: the linking mechanism and the complications. *Archives of Medical Science*, 4:851–863, 2017. ISSN 1734-1922. doi: 10.5114/aoms.2016.58928.
13. L. Fan, H. Li, J. Zhuo, Y. Zhang, J. Wang, L. Chen, Z. Yang, C. Chu, S. Xie, A.R. Laird, P.T. Fox, S.B. Eickhoff, C. Yu, and T. Jiang. The Human Brainnetome Atlas: A New Brain Atlas Based on Connectional Architecture. *Cerebral Cortex*, 26(8):3508–3526, 8 2016. ISSN 1047-3211. doi: 10.1093/cercor/bhw157.
14. C.R. Figley, J.S.A. Asem, E.L. Levenbaum, and S.M. Courtney. Effects of body mass index and body fat percent on default mode, executive control, and salience network structure and function. *Frontiers in Neuroscience*, 10(June):1–23, 2016. ISSN 1662-453X. doi: 10.3389/fnins.2016.00234.
15. M.F. Folstein, S.E. Folstein, and P.R. McHugh. "Mini-mental state": A practical method for grading the cognitive state of patients for the clinician. *Journal of Psychiatric Research*, 12 (3):189–198, 11 1975. ISSN 00223956. doi: 10.1016/0022-3956(75)90026-6.
16. D. Frasca, B.B. Blomberg, and R. Paganelli. Aging, obesity, and inflammatory age-related diseases. *Frontiers in Immunology*, 8(DEC):1–10, 2017. ISSN 16643224. doi: 10.3389/fimmu.2017.01745.
17. K. J. Friston, P. Rotshtein, J. J. Geng, P. Sterzer, and R. N. Henson. A critique of functional localisers. *Neuroimage*, 30(4):1077–87, 2016.
18. I. García-García, A. Narberhaus, I. Marqués-Iturria, M. Garolera, A. Rădoi, B. Segura, R. Pueyo, M. Ariza, and M. A. Jurado. Neural Responses to Visual Food Cues: Insights from Functional Magnetic Resonance Imaging. *European Eating Disorders Review*, 21(2): 89–98, 3 2013. ISSN 10724133. doi: 10.1002/erv.2216.
19. I. García-García, M.A. Jurado, M Garolera, B Segura, I Marqués-Iturria, R Pueyo, M Vernet-


DRAFT

Vernet, M.J. Sender-Palacios, R Sala-Llonch, M Ariza, A Narberhaus, and C Junqué. Functional connectivity in obesity during reward processing. *NeuroImage*, 66:232–239, 2 2013. ISSN 10538119. doi: 10.1016/j.neuroimage.2012.10.035.

20. I. García-García, M.A. Jurado, M. Garolera, B. Segura, R. Sala-Llonch, I. Marqués-Iturria, R. Pueyo, M.J. Sender-Palacios, M. Vernet-Vernet, A. Narberhaus, M. Ariza, and C. Junqué. Alterations of the salience network in obesity: A resting-state fMRI study. *Human Brain Mapping*, 34(11):2786–2797, 11 2013. ISSN 10659471. doi: 10.1002/hbm.22104.
21. I. García-García, M.A. Jurado, M. Garolera, I. Marqués-Iturria, A. Horstmann, B. Segura, R. Pueyo, M.J. Sender-Palacios, M. Vernet-Vernet, A. Villringer, C. Junqué, D.S. Margulies, and J. Neumann. Functional network centrality in obesity: A resting-state and task fMRI study. *Psychiatry Research: Neuroimaging*, 233(3):331–338, 9 2015. ISSN 09254927. doi: 10.1016/j.pscychresns.2015.05.017.
22. I. García-García, A. Michaud, M. Dadar, Y. Zeighami, S. Neseliler, D.L Collins, A.C. Evans, and A. Dagher. Neuroanatomical differences in obesity: meta-analytic findings and their validation in an independent dataset. *International Journal of Obesity*, 9, 7 2018. ISSN 0307-0565. doi: 10.1038/s41366-018-0164-4.
23. L. Geerligs, R.J. Renken, E. Saliasi, N.M. Maurits, and M.M. Lorist. A Brain-Wide Study of Age-Related Changes in Functional Connectivity. *Cerebral Cortex*, 25(7):1987–1999, 7 2015. ISSN 1460-2199. doi: 10.1093/cercor/bhu012.
24. P. Geha, G. Cecchi, Todd C.R., C. Abdallah, and D.M. Small. Reorganization of brain connectivity in obesity. *Human Brain Mapping*, 38(3):1403–1420, 3 2017. ISSN 10659471. doi: 10.1002/hbm.23462.
25. L. Griffanti, G. Douaud, J. Bijsterbosch, S. Evangelisti, F. Alfaro-Almagro, M.F. Glasser, E.P. Duff, S. Fitzgibbon, R. Westphal, D. Carone, C.F. Beckmann, and S.M. Smith. Hand classification of fMRI ICA noise components. *NeuroImage*, 154(June 2016):188–205, 2017. ISSN 10959572. doi: 10.1016/j.neuroimage.2016.12.036.
26. I. Marqués-Iturria, R. Pueyo, M. Garolera, B. Segura, C. Junqué, I. García-García, M.J. Sender-Palacios, M. Vernet-Vernet, A. Narberhaus, M. Ariza, and M.A. Jurado. Frontal cortical thinning and subcortical volume reductions in early adulthood obesity. *Psychiatry Research: Neuroimaging*, 214(2):109–115, 11 2013. ISSN 09254927. doi: 10.1016/j.pscychresns.2013.06.004.
27. T.J. Haight, R.N. Bryan, G. Erus, C. Davatzikos, D.R. Jacobs, M. D'Esposito, C.E. Lewis, and L.J. Launer. Vascular risk factors, cerebrovascular reactivity, and the default-mode brain network. *NeuroImage*, 115:7–16, 2015. ISSN 10959572. doi: 10.1016/j.neuroimage.2015.04.039.
28. I. Marqués-Iturria, M. Garolera, R. Pueyo, B. Segura, I. Hernan, I. García-García, C. Sánchez-Garre, M. Vernet-Vernet, M.J. Sender-Palacios, A. Narberhaus, M. Ariza, C. Junqué, and M.A. Jurado. The interaction effect between BDNF val66met polymorphism and obesity on executive functions and frontal structure. *American Journal of Medical Genetics Part B: Neuropsychiatric Genetics*, 165(3):245–253, 4 2014. ISSN 15524841. doi: 10.1002/ajmg.b.32229.
29. I. Marqués-Iturria, L.H. Scholtens, M. Garolera, R. Pueyo, I. García-García, P. González-Tartiere, B. Segura, C. Junqué, M.J. Sender-Palacios, M. Vernet-Vernet, C. Sánchez-Garre, M.A. de Reus, M.A. Jurado, and M.P. van den Heuvel. Affected connectivity organization of the reward system structure in obesity. *NeuroImage*, 111:100–106, 5 2015. ISSN 10538119. doi: 10.1016/j.neuroimage.2015.02.012.
30. L. Moreno-Lopez, O. Contreras-Rodriguez, C. Soriano-Mas, E.A. Stamatakis, and A. Verdejo-Garcia. Disrupted functional connectivity in adolescent obesity. *NeuroImage: Clinical*, 12:262–268, feb 2016. ISSN 22131582. doi: 10.1016/j.nicl.2016.07.005.
31. M. Mongraw-Chaffin, M. C. Foster, R. R. Kalyani, D. Vaidya, G. L. Burke, M. Woodward, and C. A. M. Anderson. Obesity Severity and Duration Are Associated With Incident Metabolic Syndrome: Evidence Against Metabolically Healthy Obesity From the Multi-Ethnic Study of Atherosclerosis. *The Journal of Clinical Endocrinology Metabolism*, 101(11):4117–4124, 2016.
32. J. Ottino-González, M.A. Jurado, I. García-García, X. Caldú, X. Prats-Soteras, E. Tor, M.J. Sender-Palacios, and M. Garolera. Allostatic load and executive functions in overweight adults. *Psychoneuroendocrinology*, 106(April):165–170, 8 2019. ISSN 03064530. doi: 10.1016/j.psyneuen.2019.04.009.
33. J. Ottino-González, M A Jurado, I. García-García, B Segura, I. Marqués-Iturria, M. J. Sender-Palacios, E. Tor, X. Prats-Soteras, X. Caldú, C. Junqué, O. Pasternak, and M. Garolera. Allostatic load and disordered white matter microstructure in overweight adults. *Scientific Reports*, 8(1):15898, 12 2018. ISSN 2045-2322. doi: 10.1038/s41598-018-34219-8.
34. J. Ottino-González, M.A. Jurado, I. García-García, B. Segura, I. Marqués-Iturria, M.J. Sender-Palacios, E. Tor, X. Prats-Soteras, X. Caldú, C. Junqué, and M. Garolera. Allostatic Load Is Linked to Cortical Thickness Changes Depending on Body-Weight Status. *Frontiers in Human Neuroscience*, 11(December):1–11, 12 2017. ISSN 1662-5161. doi: 10.3389/fnhum.2017.00639.
35. S. Palmqvist, M. Schöll, O. Strandberg, N. Mattsson, E. Stomrud, H. Zetterberg, K. Blennow, S. Landau, W. Jagust, and O. Hansson. Earliest accumulation of $\beta$-amyloid occurs within the default-mode network and concurrently affects brain connectivity. *Nature Communications*, 8(1):1214, 12 2017. ISSN 2041-1723. doi: 10.1038/s41467-017-01150-x.
36. R.H.R. Pruim, M. Mennes, D. van Rooij, A. Llera, J.K. Buitelaar, and C.F. Beckmann. ICA-AROMA: A robust ICA-based strategy for removing motion artifacts from fMRI data. *NeuroImage*, 112:267–277, 5 2015. ISSN 10538119. doi: 10.1016/j.neuroimage.2015.02.064.
37. R Core Team. R: A Language and Environment for Statistical Computing, 2018.
38. J. Repple, N. Opel, S. Meinert, R. Redlich, T. Hahn, N.R. Winter, C. Kaehler, D. Emden, R. Leenings, D. Grotegerd, D. Zaremba, Christian Bürger, Katharina Förster, Katharina Dohm, Verena Enneking, Elisabeth J. Leehr, Joscha Böhnlein, Greta Karliczek, Walter Heindel, Harald Kugel, J. Bauer, V. Arolt, and U. Dannlowski. Elevated body-mass index is associated with reduced white matter integrity in two large independent cohorts. *Psychoneuroendocrinology*, 91(March):179–185, 5 2018. ISSN 03064530. doi: 10.1016/j.psyneuen.2018.03.007.
39. L. Ronan, A.F. Alexander-Bloch, K. Wagstyl, S. Farooqi, C. Brayne, L.K. Tyler, Cam-CAN, P.C. Fletcher, Cam-CAN, and P.C. Fletcher. Obesity associated with increased brain age from midlife. *Neurobiology of aging*, 47:63–70, 7 2016. ISSN 1558-1497. doi: 10.1016/j.neurobiolaging.2016.07.010.
40. M. Rubinov and O. Sporns. Complex network measures of brain connectivity: Uses and interpretations. *NeuroImage*, 52(3):1059–1069, 9 2010. ISSN 10538119. doi: 10.1016/j.neuroimage.2009.10.003.
41. R. Sala-Llonch, C. Junqué, E.M. Arenaza-Urquijo, D. Vidal-Piñeiro, C. Valls-Pedret, E.M. Palacios, S. Domènech, A. Salvà, N. Bargalló, and D. Bartrés-Faz. Changes in whole-brain functional networks and memory performance in aging. *Neurobiology of Aging*, 35(10):2193–2202, 10 2014. ISSN 01974580. doi: 10.1016/j.neurobiolaging.2014.04.007.
42. R. Sala-Llonch, D. Bartrés-Faz, and C. Junqué. Reorganization of brain networks in aging: a review of functional connectivity studies. *Frontiers in Psychology*, 6(May):1–11, 5 2015. ISSN 1664-1078. doi: 10.3389/fpsyg.2015.00663.
43. J.S. Siegel, B.A. Seitzman, L.E. Ramsey, M. Ortega, E.M. Gordon, N.U.F. Dosenbach, S.E. Petersen, G.L. Shulman, and M. Corbetta. Re-emergence of modular brain networks in stroke recovery. *Cortex*, 101:44–59, 2018. ISSN 19738102. doi: 10.1016/j.cortex.2017.12.019.
44. S.J. Spencer, H. D'Angelo, A. Soch, L.R. Watkins, S.F. Maier, and R.M. Barrientos. High-fat diet and aging interact to produce neuroinflammation and impair hippocampal- and amygdalar-dependent memory. *Neurobiology of Aging*, 58:88–101, 10 2017. ISSN 0197-4580. doi: 10.1016/J.NEUROBIOLAGING.2017.06.014.
45. J.M. Spielberg, N. Sadeh, E.C. Leritz, R.E. McGlinchey, W.P. Milberg, J.P. Hayes, and D.H. Salat. Higher serum cholesterol is associated with intensified age-related neural network decoupling and cognitive decline in early- to mid-life. *Human Brain Mapping*, 38(6):3249–3261, 2017. ISSN 10970193. doi: 10.1002/hbm.23587.
46. O Sporns. Network attributes for segregation and integration in the human brain. *Current opinion in neurobiology*, 1 2013. ISSN 1873-6882; 0959-4388. doi: 10.1016/j.conb.2012.11.015;10.1016/j.conb.2012.11.015.
47. O. Sporns. Structure and function of complex brain networks. *Dialogues in clinical neuroscience*, 15(3):247–262, 9 2013. ISSN 1958-5969.
48. J.R. Tregellas, K.P. Wylie, D.C. Rojas, J. Tanabe, J. Martin, E. Kronberg, D. Cordes, and M.A. Cornier. Altered Default Network Activity in Obesity. *Obesity (Silver Spring, Md.)*, 19(21):2316–2321, 6 2011. ISSN 1930-7381; 1930-7381. doi: 10.1038/oby.2011.119.
49. I.P. Tzanetakou, N.L. Katsilambros, A. Benetos, D.P. Mikhailidis, and D.N. Perrea. "Is obesity linked to aging?": adipose tissue and the role of telomeres. *Ageing research reviews*, 11(2):220–9, 5 2012. ISSN 1872-9649.
50. M.N. Valcarcel-Ares, Z. Tucsek, T. Kiss, C.B. Giles, S. Tarantini, A. Yabluchanskiy, P. Balasubramanian, T. Gautam, V. Galvan, P. Ballabh, A. Richardson, W.M. Freeman, J.D. Wren, F. Deak, Z. Ungvari, and A. Csiszar. Obesity in Aging Exacerbates Neuroinflammation, Dysregulating Synaptic Function-Related Genes and Altering Eicosanoid Synthesis in the Mouse Hippocampus: Potential Role in Impaired Synaptic Plasticity and Cognitive Decline. *The Journals of Gerontology: Series A*, 74(3):290–298, 2 2019. ISSN 1079-5006. doi: 10.1093/gerona/gly127.
51. M.P. van den Heuvel and O. Sporns. Network hubs in the human brain. *Trends in cognitive sciences*, 17(12):683–96, 12 2013. ISSN 1879-307X. doi: 10.1016/j.tics.2013.09.012.
52. K.H. Wade, D. Carslake, N. Sattar, S.G. Davey, and N.J. Timpson. BMI and Mortality in UK Biobank: Revised Estimates Using Mendelian Randomization. *Obesity*, 26(11):1796–1806, 11 2018. ISSN 1930-7381. doi: 10.1002/oby.22313.
53. D Wechsler. *WAIS III. Escala de Inteligencia de Wechsler para adultos III (adaptación española ed.)*, volume adaptación. TEA Editores S.A., Madrid, 1999.
54. D Wechsler. *WISC-IV: Escala de Inteligencia de Wechsler para Niños-IV (2da edición)*. Madrid, 2007.
55. G.S. Wig. Segregated Systems of Human Brain Networks. *Trends in Cognitive Sciences*, 21(12):981–996, 2017. ISSN 1879307X. doi: 10.1016/j.tics.2017.09.006.
56. World Health Organization. BMI classification, 2012.
57. World Health Organization. World Report on Ageing and Health. Technical report, 2015.
58. Regional Office for Europe World Health Organization. Obesity: Data and statistics. Technical report, 2017.
59. R. Zhang, F. Beyer, L. Lampe, T. Luck, S.G. Riedel-Heller, M. Loeffler, M.L. Schroeter, M. Stumvoll, A. Villringer, and A.V. Witte. White matter microstructural variability mediates the relation between obesity and cognition in healthy adults. *NeuroImage*, 172(February):239–249, 2018. ISSN 10959572. doi: 10.1016/j.neuroimage.2018.01.028.

DRAFT

## Supplementary Material

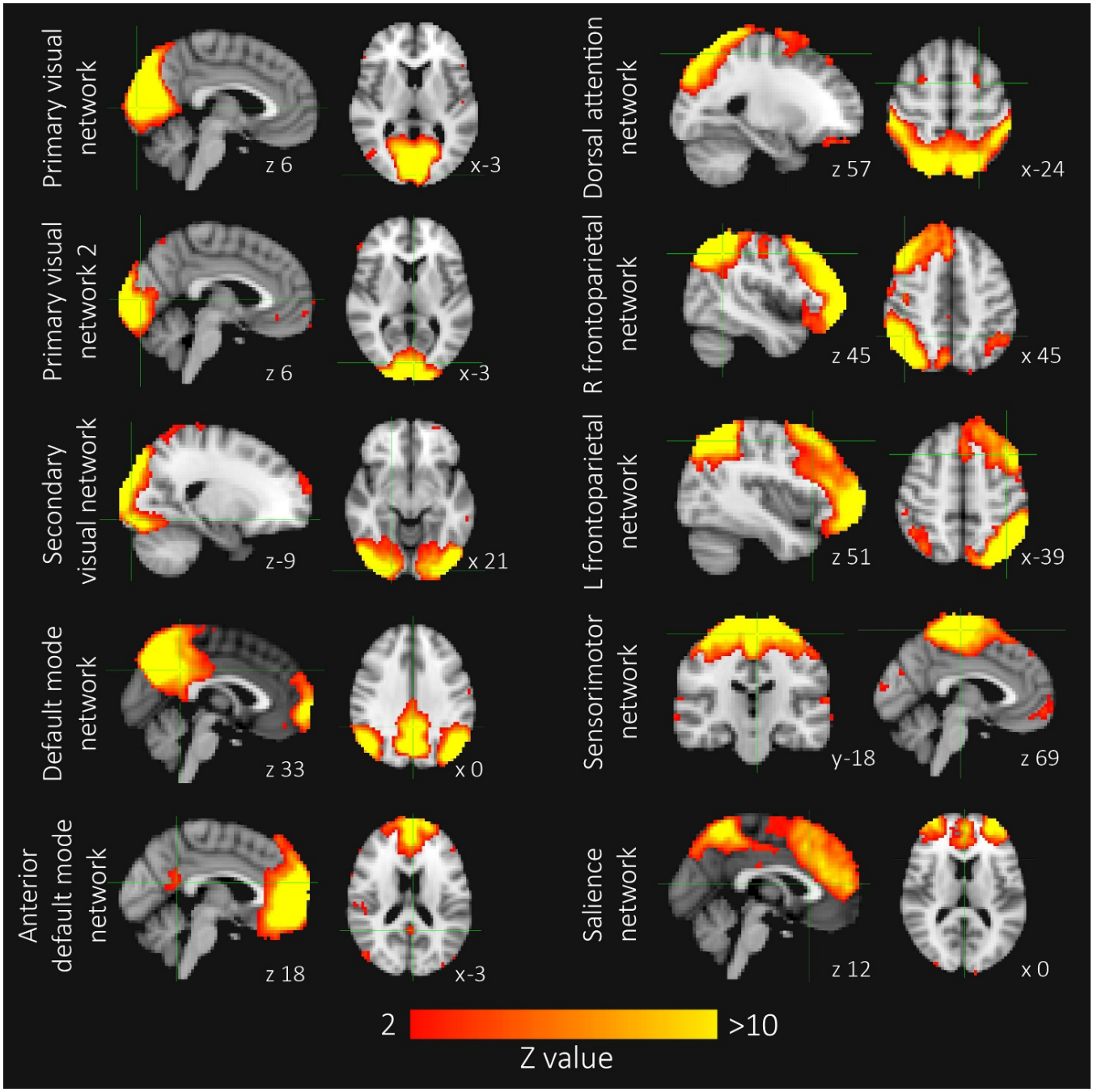


**Supplementary Figure 1**. Plots disclose the spatial maps corresponding to 10 networks of interest characterized through independent component analysis. The x, y or z MNI coordinates of the slices shown are indicated. In coronal and axial slices, the right hemisphere is displayed on the left side of the image. R: right; L: left.

| | | | | | |
|---|---|---|---|---|---|
| **Primary visual network** | | | | | |
| Cun_L_5_2 | Cun_L_5_4 | Cun_L_5_5 | Cun_R_5_2 | Cun_R_5_3 | Cun_R_5_5 |
| sOcG_L_2_1 | sOcG_R_2_1 | | | | |
| **Primary visual network 2** | | | | | |
| Cun_L_5_1 | Cun_L_5_3 | Cun_R_5_1 | OcG_R_4_3 | | |
| **Secondary visual network** | | | | | |
| FuG_L_3_2 | FuG_R_3_2 | OcG_L_4_1 | OcG_L_4_2 | OcG_L_4_3 | OcG_L_4_4 |
| OcG_R_4_1 | OcG_R_4_2 | OcG_R_4_4 | sOcG_L_2_2 | | |
| **Anterior default mode network** | | | | | |
| CG_L_7_7 | CG_R_7_7 | OrG_L_6_1 | OrG_L_6_4 | OrG_R_6_1 | SFG_L_7_3 |
| SFG_L_7_7 | SFG_R_7_7 | | | | |
| **Dorsal attention network** | | | | | |
| IPL_L_6_1 | IPL_R_6_1 | IPL_R_6_3 | ITG_L_7_5 | ITG_R_7_2 | ITG_R_7_5 |
| sOcG_R_2_2 | SPL_L_5_1 | SPL_L_5_2 | SPL_L_5_4 | SPL_R_5_1 | SPL_R_5_2 |
| SPL_R_5_3 | SPL_R_5_5 | | | | |
| **Default mode network** | | | | | |
| CG_L_7_1 | CG_R_7_1 | IPL_L_6_5 | IPL_R_6_5 | Pcun_L_4_1 | Pcun_L_4_3 |
| Pcun_L_4_4 | Pcun_R_4_1 | Pcun_R_4_3 | Pcun_R_4_4 | pSTS_L_2_2 | |
| **Left frontoparietal network** | | | | | |
| IFG_L_6_1 | IFG_L_6_2 | IFG_L_6_3 | IFG_L_6_4 | IFG_L_6_6 | IPL_L_6_2 |
| ITG_L_7_2 | ITG_L_7_6 | MFG_L_7_2 | MFG_L_7_4 | MFG_L_7_5 | MFG_L_7_6 |
| OrG_L_6_2 | OrG_L_6_3 | OrG_L_6_6 | SFG_L_7_2 | SPL_L_5_5 | |
| **Right frontoparietal network** | | | | | |
| IFG_R_6_2 | IFG_R_6_3 | IPL_R_6_2 | ITG_R_7_6 | MFG_R_7_4 | MFG_R_7_5 |
| MFG_R_7_6 | MTG_R_4_1 | OrG_R_6_2 | OrG_R_6_3 | OrG_R_6_6 | SFG_R_7_2 |
| SFG_R_7_3 | | | | | |
| **Salience network** | | | | | |
| CG_L_7_3 | CG_R_7_3 | IPL_L_6_3 | IPL_L_6_4 | IPL_R_6_4 | MFG_L_7_1 |
| MFG_L_7_3 | MFG_R_7_1 | MFG_R_7_3 | PCL_R_2_1 | Pcun_L_4_2 | SFG_L_7_1 |
| SFG_L_7_6 | SFG_R_7_1 | SFG_R_7_6 | SPL_L_5_3 | | |
| **Sensorimotor network** | | | | | |
| PCL_L_2_1 | PCL_L_2_2 | PCL_R_2_2 | Pcun_R_4_2 | PoG_L_4_4 | PoG_R_4_4 |
| PrG_L_6_3 | PrG_L_6_4 | PrG_R_6_2 | PrG_R_6_3 | PrG_R_6_4 | SFG_L_7_4 |
| SFG_L_7_5 | SFG_R_7_4 | SFG_R_7_5 | SPL_R_5_4 | | |
| **Medial temporal network** | | | | | |
| Amyg_L_2_1 | Amyg_L_2_2 | Amyg_R_2_1 | Amyg_R_2_2 | Hipp_L_2_1 | Hipp_L_2_2 |
| Hipp_R_2_1 | Hipp_R_2_2 | | | | |
| **Striatal thalamic network** | | | | | |
| Str_L_6_1 | Str_L_6_2 | Str_L_6_3 | Str_L_6_4 | Str_L_6_5 | Str_L_6_6 |
| Str_R_6_1 | Str_R_6_2 | Str_R_6_3 | Str_R_6_4 | Str_R_6_5 | Str_R_6_6 |
| Tha_L_8_1 | Tha_L_8_2 | Tha_L_8_3 | Tha_L_8_4 | Tha_L_8_5 | Tha_L_8_6 |
| Tha_L_8_7 | Tha_L_8_8 | Tha_R_8_1 | Tha_R_8_2 | Tha_R_8_3 | Tha_R_8_4 |
| Tha_R_8_5 | Tha_R_8_6 | Tha_R_8_7 | Tha_R_8_8 | | |

**Supplementary Table 1**. Brainnetome atlas regions (http://atlas.brainnetome.org/) assigned to each of the 12 brain networks of interest.

DRAFT

| | OB adult | HW adult | Senior | OB young | HW young |
|---|---|---|---|---|---|
| *Modularity* | 0.45 (0.80) | -0.12 (1.17) | -0.33 (0.82) | 0.25 (0.99) | -0.24 (0.97) |
| *Path length* | 0.08 (0.83) | -0.19 (0.85) | 0.12 (1.27) | 0.19 (1.04) | -0.18 (0.94) |
| *Mean degree* | -0.46 (0.65) | 0.24 (1.17) | 0.21 (0.96) | -0.27 (0.69) | 0.26 (1.18) |
| *Mean strength* | -0.42 (0.67) | 0.26 (1.18) | 0.14 (0.96) | -0.27 (0.81) | 0.26 (1.11) |

**Supplementary Table 2.** Mean and standard deviation of graph-based parameters across groups (z-scores). OB = Participants with obesity, HW = Healthy-weight individuals.

DRAFT